DEVELOPING WINTER RESIDENTIAL DEMAND RESPONSE STRATEGIES FOR ELECTRIC SPACE HEATING

Leduc Marie-Andrée[1], Daoud Ahmed[1], and Le Bel Célyn[1]
[1]Laboratoire des technologies de l'énergie d'Hydro-Québec, Shawinigan, Qc, Canada

ABSTRACT

The objective of this paper is to present space heating strategies leading to a load reduction during critical periods on the grid but also taking into account the occupant thermal comfort in order to make them acceptable. Using TRNSYS, three types of strategies were investigated: lowering the thermostat setpoint, storing heat in the building thermal mass during off-peak hours and lowering the setpoint during critical periods, and limiting the available power to baseboards. Results show that the strategies can save up to 7 kW per residence which corresponds to 90% of the reference heating load of the average residence.

INTRODUCTION

In the province of Quebec, Canada, electricity is provided by the government owned utility, Hydro-Quebec, which produces mainly from renewables (98% of its production). The region's electric grid peaks in winter; around 38 000 MW as of 2011. All-electric households are largely responsible for this peak demand. More than two third of households use electricity as their exclusive source of energy and are therefore defined as all-electric (AE) households. For approximately 87% of these AE households, space heating is done using electric baseboards, located in each heated room of the house, and controlled by their own line-voltage thermostat. During peak hours, the space heating load of AE households can account for up to 80% of their total load. The shape of the region's demand profile is strongly coincident with the demand profile from these customers. For the commercial and institutional sector (CI), electricity is the main source of energy for space heating for 60% of the utility's customers, of which 75% have baseboards and room thermostats similar to the equipment used in the residential sector. For the winter's highest peak hour, the combined space heating load, from the residential and CI sectors, represents 40% of the total electric utility peak load. It is expected that the installation of electric space heating will increase over the coming years due to their low initial and operating cost, hence reducing the gap between the available resources and the demand during peak hours.

Demand response involving residential AE households could possibly relieve the electric grid and should therefore be investigated. Many studies involving the residential sector have been done over the years. California's vast *Statewide Pricing Pilot* (SPP) (CRA, 2005) and Oregon's Olympic Peninsula (PNNL, 2007) are probably the most well-known. From the detailed analysis of the *SPP* data (Herter et *al*., 2007), it was found that automation had a great effect on load reduction, greater than price signal alone. Since electric space heating is the most important load during peak hours, it therefore seems logical to focus this study on possible automated control strategies for decentralised heating equipments. It has been decided that this study should not involve the use of thermal storage devices or alternative fuel sources in order to reduce the complexity and cost of the implementation of these strategies. This would make them applicable to all AE households since only their line-voltage thermostats would have to be replaced by communicating thermostats. These strategies must lead to a peak heating load reduction but must also take into account the occupant thermal comfort in order to make them acceptable. The feasibility of such strategies has to be demonstrated for light thermal mass wood-framed buildings typical for houses in Quebec.

In the past few years, many studies have been done to evaluate the effect of controlling cooling equipments on the building's total peak load. Most of the work found in literature has been focussing on commercial and institutional buildings. Studies have been done on the reduction of the cooling load using night cooling and on the effect of thermal mass and thermal storage devices (Braun et *al*, 2003; Yang et *al*, 2008; LBNL, 2006; Yin et *al*, 2010). Others have focused on optimal control of setpoints and storage (Lee et *al*., 2008; Henze et al, 2005). Katipamula (Katipamula et *al*, 2006) and Reddy (Reddy et *al*, 1991) have studied control strategies for HVAC equipment in residential buildings.

Very few studies are available on winter peak reduction obtained by controlling the space heating equipment. Persson (Persson et *al*, 2005) have explored space heating peak load reduction but their solutions involved the use of substitution fuel

sources. Lu (Lu et *al*, 2005) has focused on the global effect of controlling thermostatically controlled appliances on the electric grid but not on the effect of this control on occupant thermal comfort. Oregon's Portland General Electric Co. had a pilot project in 2004 on direct load control for electric space heating which showed that residential customers could reduce their peak load by 0.48 to 0.73 kW by reducing their space heating setpoint by 2-3 °C for 2 to 3 hours without much complaints (PGE, 2004). The Olympic Peninsula pilot project included the control of resistive heating equipment but only for homes controlled by one or at most two thermostats. The results of this pilot study showed that a significant part of the overall load reduction due to price increase came from a decrease or shift in space heating load (PNNL, 2007).

SIMULATION

TRNSYS 16 was selected to create the building energy model. It is widely used by the building simulation scientific community, particularly in research. It has been used to evaluate peaking load control by others (Henze et *al*, 2005, Persson et *al*, 2005, Braun et *al*, 2002). Indeed, this tool offers great flexibility. It is user-friendly and allows the incorporation of a wide range of systems through its modular ('TYPE') structure. The TYPE56, the model of multizone building, was used to model the house described in the next section. TYPE56 is a non-geometric model with an air node per thermal zone. The flow of heat received by the node is the sum of convective and radiative flows from the adjacent surfaces, gains by infiltration, ventilation, internal heat gains as well as air coupling from other zones. This detailed multizone building model was chosen in order to simulate complex space heating load strategies adapted to the decentralized heating equipment typical of the type of housing studied.

The time step used for the simulations vary greatly depending of the model. The choice of 5 min seems reasonable. A smaller time step would proportionally increase the calculation time and would not significantly improve the solution as demonstrated later. The meteorological file used for the simulation covers two years, from January 1st 2003 to December 31th 2004. In fact, the year 2004 has recorded a peak demand of 36 268 MW on Hydro-Quebec grid on January 15th, for an outside dry bulb peak temperature of -30 °C. All strategies are simulated on January 15th only.

The architecture of the modeled building is based on the twin experimental houses built on the site of the Laboratoire des technologies de l'énergie d'Hydro-Québec (LTE). The building has a total heated area of 2034 sq. ft. (189 m^2) including a heated garage of 312 sq. ft. (29 m^2). The total fenestration area is 205 sq. ft. (19 m^2). In this model, the orientation of the building facade is facing north. Table 1 shows the details of the building's structure.

Table 1
Building Characteristics

Wall	Material	Thickness (cm)	Thermal resistance[1] (K·m2 / W)
External Wall - sky view factor = 0.5			3.2
	Gypsum board	12.7	
	Insulation	127	
	Sheathing	12.7	
	Air vertical	-	
	Vinyl	0	
External Wall - sky view factor = 0.5			3.3
	Gypsum board	12.7	
	Insulation	127	
	Sheathing	12.7	
	Air vertical	-	
	Brick	102	
Roof - sky view factor = 0.9 (surf37°) et 0.85 (surf46°)			5.4
	Gypsum board	12.7	
	Insulation	152	
	Wool batts Insulation	73	
	Plywood	12.7	
	Roofing	-	
Vertical Foundations - sky view factor = 0.5			2.3
	Gypsum board	12.7	
	Extruded polystyrene	50	
	Concrete	254	
Horizontal Foundations			1.6
	Carpet	25	
	Extruded polystyrene	25	
	Concrete	102	
Internal Wall (between house and garage)			2.9
	Gypsum board	12.7	
	Insulation	127	
	Gypsum board	12.7	

[1] From U-value evaluated by TRNSYS.

Insulation levels were primarily taken from Hydro-Quebec projects (HQ, 1993) (Millette et *al*., 2004) and from Novoclimat technical requirements and guidelines (AEE, 2010). Occupation schedules were generated using the forcing functions available in TRNSYS in steps of 5 min. Occupation schedules are representative of a family of four persons. A type of activity is assigned to each area and determines the instant heat gains from the occupants (sensitive and latent), according to the standard ISO 7730.

Lighting effects were modeled by an internal heat gain equivalent to 5 or 10 W/m^2 (100% radiative). These assumptions are due to the choice of compact fluorescent lamps installed in the building. This gain is applied according to the corresponding occupational schedule, which is valid for the winter period which is the focus of this study.

We consider only the internal heat gain of equipments having a demand of more than 100 W (refrigeration/freezing equipments are excluded).

Hence, the following are considered: cooking range, televisions and domestic hot water electric heaters. Clothes dryer was excluded since a large portion of the consumed energy is evacuated outside.

Infiltration rates are given in air change per hour (ACH) and are representative of natural ventilation, as required in the model. Infiltration rates are assumed constant and applied to every zone having an outdoor surface. In this study we considered an infiltration rate of 0.213 ACH.

Table 2 summarizes all the heat gains in the model.

Table 2
Heat gains

Simulation Year	Infiltrations (kWh)	Internal gains (kWh)	Solar gains (kWh)
2003	-6 094	4 185	6 632
2004	-6 082	4 185	6 751

Equipments	(W)
Cooking range	450
TV	160
DHW	100

Thermal comfort is evaluated according to ISO 7730 standard. This calculation is included in the TYPE56 and is used to evaluate the comfort of the occupants of the modeled building. Comfort criteria were therefore added in the occupied areas to determine the viability of some load management strategies. The insulation values of clothing (English clothing factor) were chosen based on clothing in winter, period which is of interest in this project. Only areas with a schedule of occupation have been considered. The air velocity is estimated at 0.1 m/s, which is representative of air flows in residential homes.

To bring the effect of thermal mass to the building representative of houses in Quebec, two changes were made. Firstly, the capacitance of air (C_p) was changed to $C_p = 30 \times V_{zone}$ for all areas except the attic and the garage. This rule is consistent with that found in the literature (Charron et *al.*, 2007). This change was made to obtain short time constants of the same order of magnitude as those obtained experimentally (Gunther, 2001). Secondly, internal walls were added in the main occupied areas. These internal walls are wooden surfaces of 25 cm thick, with a coefficient of convection for the internal walls of 11 kJ/hm^{2}K. This addition allowed the long time constants to be of the same order of magnitude as those obtained experimentally.

Equipment that could have an impact on the heat balance of the building has been neglected for reasons of simplification of the model and the calculation time reduction. For example, a number of small appliances having a low frequency of use were not modelled although they contribute to reduce the heating load by producing internal gains. Local ventilation (kitchen hoods and bathroom fans) was not modelled because its frequency of use is low. Latent internal gains have not been quantified for the household appliances included in the model (e.g. the cooking range).

Electric baseboard is the only heating technology used in the modeled building. Electric baseboard heaters are located in every room of the house and sized as those in LTE's experimental houses. The total installed capacity is 17 kW including the garage. A fraction of the installed capacity may be considered as a gain by radiation that will apply to all surfaces of the area. This has the effect of reducing the portion of heating which is directly transmitted to the air by convection, as is the case in reality with the plume of warm air which warms the surface above the electric baseboard. However, all of the surfaces of the zone enjoy gain while in reality, this is the case for only one of the surfaces. This would increase the temperature of the surfaces together, so to modify the transfer of heat between these surfaces and the adjacent area. The effect should be negligible.

The TYPE56 already integrates a perfect control of heating, namely that the demand is equal to the heating load at any time. This demand can be limited to the installed capacity. This type of control is a reasonable approximation for an electronic thermostat having proportional control. The thermostats' setpoint is constant at 21 °C except for garage which is kept at 0 °C.

VALIDATION

In order to validate the model, the annual energy consumption, apparent UA value and time constants for the building have been compared to either experimental data or other models for similar buildings.

The apparent UA value is defined by Equation 1 and derived experimentally from Equation 2 using night time ($E_{solar} = 0$) winter data (to approximate a permanent regime).

$$UA_{\text{apparent}}(\Delta T) = UA_{\text{enveloppe}}(\Delta T) + m_{\text{infiltration}} C_p(\Delta T) \quad \text{Eq 1}$$

$$E_{\text{heating}} = UA_{\text{apparent}}(\Delta T) \cdot t - E_{\text{internal}} - E_{\text{solar}} \quad \text{Eq 2}$$

Table 3 presents these values for the two years studied. Experimental data was taken from Gunther (Gunther, 2001) and the simulation data from Moreau (Moreau et *al.*, 1994).

Table 3
Building Characteristics

Building	Annual heating (kWh)	UA_{app} (W/C)	τ_c	τ_l	C_c	C_l
			(h)		(kWh /C)	
Model	(2003) 14010 (2004) 13740	154	43	58	6.6	8.9
Experiental data		158[1]	36[2]	54[2]	6.0[2]	8.9[2]
Simulation data[3]	13803					

[1]building 1993, [2]all buildings average,
[3]RSI exterior wall = 3.52, ELA = 319 cm^2

To evaluate the time constants of the building, two power cuts have been simulated for each year (release test). The evolution of the average temperature of the building during the release test is shown to follow an exponential decrease and can be represented by a two time constants lumped capacitance model. The short time constant is evaluated by taking the data for the first three hours of the release test and the long time constant with the remaining data, Equation 3 is used to calculate the thermal capacity *C*.

$$\ln\left[\frac{T_{\text{int},t0}-T_{\text{ext}}}{T_{\text{int},t}-T_{\text{ext}}}\right]=\frac{UA_{apparent}}{C}\cdot t=\frac{t}{\tau} \qquad \text{Eq 3}$$

The sensitivity of the model to certain parameters has been investigated; these include the internal convection coefficient, time step, thermal mass and infiltration rate. Effects on both the temperature and demand profiles have been studied for the peaking day of 2004 as this is the period of interest here.

The internal convection coefficients used in the model can have a significant impact on the load profile, therefore on the annual energy consumption. Beausoleil-Morrisson (Beausoleil-Morisson, 2002) has found that the use of an adaptive algorithm able to differentiate the surface type and conditions and use the appropriate correlation to calculate the internal convection coefficient can produce a significant difference on the annual energy consumption. This difference is greater for poorly insulated buildings.

For this model, two options have been tested. The first is the reference case which uses constant internal convection coefficients for all internal surfaces (walls and windows). The second uses TRNSYS ability to calculate the internal convection coefficient for each surface at each time step, therefore taking into account the effect of the temperature difference between the air and the surface. The coefficient is calculated using the correlation expressed by Equation 4, where A = 5,76 and n = 0,3 for vertical surfaces, A = 2,11 and n = 0,31 for horizontal surfaces if $T_{surf} \geq T_{air}$, A = 1,87 and n = 0,25 for horizontal surfaces if $T_{surf} < T_{air}$; these are the default values used by TRNSYS.

$$h_c = A\left(T_{surf}-T_{air}\right)^n \qquad \text{Eq 4}$$

Figure 1 shows that, using the default values, the calculation of the internal convection coefficients produces a difference of up to about 0,3 kW in the load profile for the period of interest (January 15th) which is small but not necessarily negligible. Hence, in future work, this aspect should be further investigated. Effect on the temperature profile is not significant.

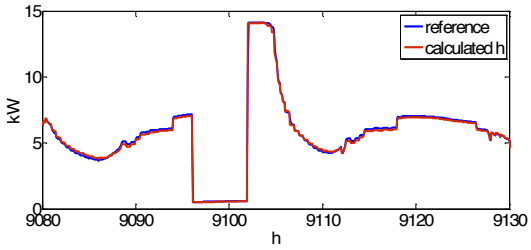

Figure 1. Effect of internal convection coefficient on the load profile

The effect of reducing the simulation time step was investigated. Figure 2 shows that there is no net advantage in reducing the time step since both cases produce similar load profiles. The temperature profiles are identical.

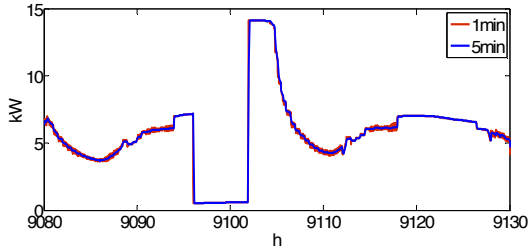

Figure 2 – Effect of time step on the load profile

As discussed earlier, both zonal capacitance and internal walls were included in the model in order to account for the thermal mass of the building. The effect of using one or the other of these methods was evaluated. Figure 3 shows that the sole use of thermal walls fails to produce a realistic temperature profile for the first hour of the release test, as the air temperature drop is too drastic. The effect of the time step is also very visible, as shown by the ripples in the slope.

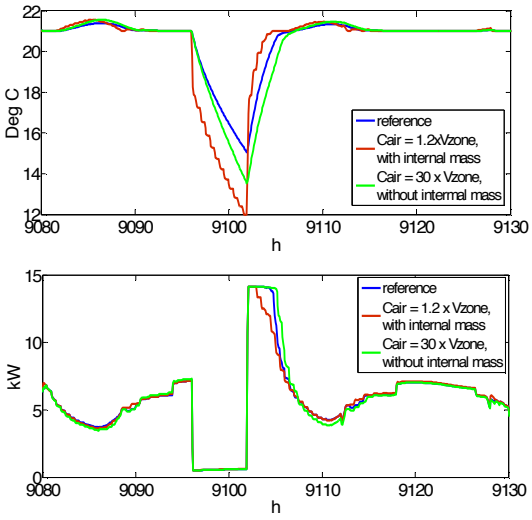

Figure 3 – Effect of thermal mass

Increase in zonal capacitance produces a far more realistic temperature profile but, according to available experimental data, the long time constant (after three hours of the release test) is slightly less than expected. Therefore, the use of both methods to add thermal mass seems to yield the best results but this would have to be validated experimentally.

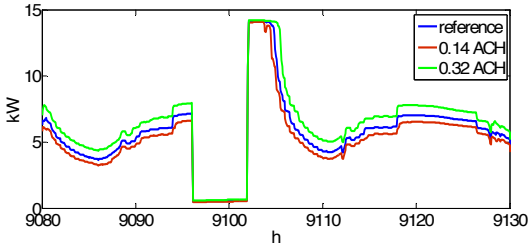

Figure 4 – Effect of infiltration on load profile

The effect of infiltration rate has been investigated. As anticipated, the effect is important as presented in Figure 4. For the annual energy consumption, an increase of the infiltration rate to 0.32 ACH produces a 14% increase in energy consumption. A decrease of the infiltration rate to 0.14 ACH produces a 9% decrease in energy consumption.

The model, using ideal heating control, seems to produce reasonable results at least for the purpose of this evaluation. Modeling of the basement could be improved by incorporating a finite difference 3-D model. The infiltration rate could easily take into account the effect of meteorological conditions such as wind speed, by incorporating Type75 (Sherman-Grimsrud model) into the model. One consideration worth noting is the fact that baseboard heating produces important temperature stratification in the zone which will in turn affects the heat transfer through floors and ceilings. This has not been taken into account.

RESULTS

Three groups of strategies were evaluated. Table 4 presents the detail of these strategies. Peak hours are defined as 6h00 to 10h00 and 16h00 to 20h00. The reference case is for a constant temperature setpoint of 21 °C.

Figures 5, 6 and 7 show the effect of the different group of strategies on the space heating load during the two daily peak periods. The 9102th hour corresponds to 6h00 on the peak day of 2004.

In order to evaluate the simulated strategies, three indicators were used. The evaluation of those indicators for the three groups of strategies is presented in Table 5 for the morning (am) and afternoon (pm) peak periods.

The first indicator, called PLR for power load ratio (Eq 5), represents the maximum power load during peak hours in comparison to the reference case.

$$PLR = \frac{P_{\max,strategy}\Big|_{t_0}^{t_{fin}}}{P_{\max,reference}\Big|_{t_0}^{t_{fin}}} \qquad \text{Eq 5}$$

It will be considered that a PLR lower than 0.8 is good (indicated by pale green shading in Table 5), between 0.8 and 0.99 acceptable. A PLR of 1.0 gives the indication that there is no power reduction during peak hours.

Table 4
Load control strategies

Strategy	
1.*Setback strategy* Setback only during peak hours, instantaneous reset algorithm	**1a**- Second floor only @ 18ºC **1b**- Basement only @ 18ºC **1c**- First floor only @ 18ºC **1d**- Second floor and basement @ 18ºC with a progressive increase of the setpoint after peak hours on the second floor over 1h until the setpoint 21ºC is reached **1e**- Strategy 1a @ 16 °C **1f**- All floor @ 18 °C **1z**- All unoccupied zones @ 18 °C
2.*Preheat strategy* Envelope thermal storage during offpeak hours and setback during peak hours, linear reset algorithm	**2a**- Setpoint @ 24 ºC from 0h00, setpoint @ 18 ºC during peak hours, setpoint increase @ 24 ºC from 10h00 until 16h00, setpoint @ 21ºC during evening **2b**- Strategy 2a with a morning preheat starting at 3h00 **2c**- Strategy 2a with setpoints @ 25 ºC instead of 24 ºC **2d**- Setpoint @ 24 ºC in unoccupied zones between 0h-6h, setpoint @ 18 ºC during peak hours, setpoint increases during one hour until 24 ºC from 10h until 16h, setpoint @ 18 ºC during peak hours setpoint @ 21ºC during evening from 20 h **2e**- strategy 2c with setpoints @ 23 ºC instead of 24 ºC
3.*Power limitation strategy* Limitation of available capacity, instantaneous reset algorithm	**3a**- 25% of the installed power available **3b**- 50% of the installed power available

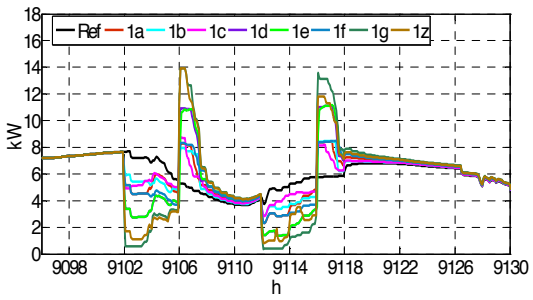

Figure 5 –Strategy 1 – setback only.

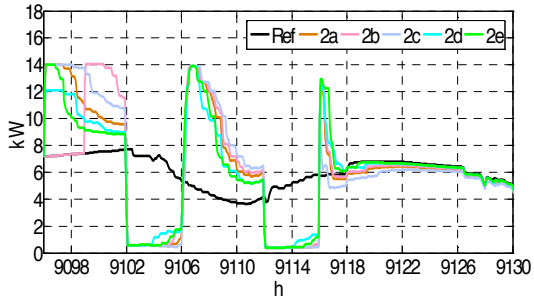

Figure 6 –Strategy 2 – preheat and setback.

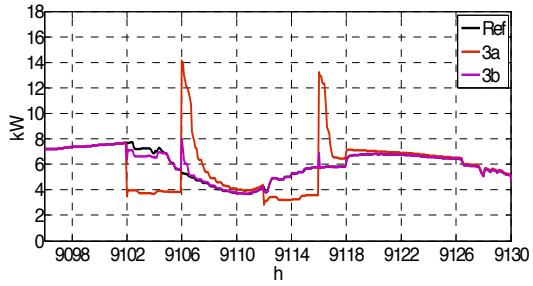

Figure 7 –Strategy 3 – power limitation.

The second indicator is the predicted percentage dissatisfied (PPD) index, a comfort indicator. The PPD indices are calculated by TRNSYS according to ISO 7730, at every time step. The PPD presented in Table 5 are for the worst instantaneous conditions observed for the occupied zones (excluding the bathroom) during the preheating and critical periods, regardless of how long these conditions may have lasted. Since the minimum air temperature in each zone is set to 18 °C, air temperature never drops below this setpoint, as shown in Figure 8.

Table 5
Indicator values for the different strategies

	AM			PM		
	PLR	**PPD**	**RR**	**PLR**	**PPD**	**RR**
1a	0.78	11.7	1.08	0.83	29.2	1.45
1b	0.77	11.7	1.03	0.74	29.1	1.46
1c	0.79	10.6	1.13	0.81	52.7	1.41
1d	0.57	11.6	1.42	0.57	29.3	1.91
1e	0.57	11.6	1.16	0.57	29.3	1.56
1f	0.67	11.7	1.08	0.64	29.2	1.45
1g	0.43	10.3	1.81	0.49	56.4	2.35
1z	0.41	11.3	1.81	0.61	29.8	2.05
2a	0.14	21.5	0.57	0.11	32.6	2.12
2b	0.22	21.5	0.58	0.11	32.6	2.17
2c	0.08	31.7	0.37	0.07	24.2	1.52
2d	0.22	19.9	0.70	0.23	35.0	2.24
2e	0.23	17.7	0.59	0.20	39.4	2.24
3a	0.52	11.7	0.00	0.62	29.3	0.00
3b	0.93	11.7	2.60	1.00	29.3	2.30

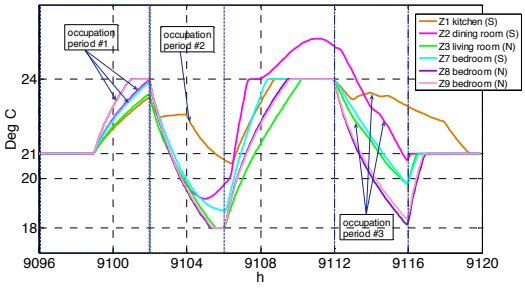

Figure 8 –Temperature profile, strategy 2b.

This first assessment of comfort is far from perfect and seems to yield questionable results, especially regarding preheating periods where little discomfort is shown even if air temperatures reach high levels (for winter clothing conditions). Future work is needed to better evaluate comfort levels associated with these strategies. Keeping in mind that these peak load control strategies would only be used for a few hours every winter, it was considered arbitrarily that a PPD lower than 50% was good (indicated by pale green shading in Table 5), between 50 and 75% acceptable and higher than 75% not acceptable.

Finally, the third indicator, called RR for reset ratio (Eq 6), represents the maximum load for the 10 min interval immediately following the end of the peak period (subscript *end*) in comparison to the reference case. This indicator evaluates the reset strategy.

$$RR = \frac{P_{\max,strategy}\Big|_{t_0}^{t_{end+2ts}}}{P_{\max,reference}\Big|_{t_0}^{t_{end+2ts}}} \qquad \text{Eq 6}$$

It will be considered that an RR lower than 1.0 is good (indicated by pale green shading in Table 5), between 1.0 and 2.0 is acceptable while higher than 2.0 is not acceptable. One must bear in mind that the RR ratio is dependent on the reset algorithm that has been adopted for the particular strategy. Strategies 1 and 3 use instantaneous reset strategies and therefore show higher RR ratio. Reset strategies could be quite easily modified to reduce the impact on the grid but might require more complex hardware equipment for field implementation.

Energy consumption for each strategy has also been evaluated, though it will not be discussed in full details in this paper. It was found that energy consumption will slightly increase for strategies involving preheat prior to setback (1-6 %); this was evaluated over a 48 hours period starting at 0h00 on the day when the strategy was applied (January 15th), after which load profiles with and without the strategy are similar again.

In terms of thermal comfort, all the strategies give good indicators for the morning peak period with a better performance for the *Setback strategy* and the *Power limitation strategy* (~11% of PPD). For the

afternoon peak period the strategies 1c and 1g are performing poorly compared to the other strategies with PPDs of 52.7% and 56.4% respectively.

In terms of PLR, all the strategies are interesting for the morning peak period except for the strategy 3b (PLR=0.93). In the afternoon period, the performance is also good for the majority of the strategies except for the 1a and 1c which give acceptable values (0.83 and 0.81) and 3b which gives a bad performance indicator (1.0). The *Preheat strategy* presents a net advantage over the other two strategies on this aspect. The largest peak reduction occurs with strategy 2c and equals 7 kW during the morning period.

In terms of RR, for the morning peak period, only the strategy 3b gives a bad indicator, the *Preheat strategy* and the strategy 3a give good RR indicators and the *Setback strategy* yields an acceptable one. For the afternoon peak period, only strategy 3a gives a good RR value, several strategies (1g, 1z, 2a, 2b, 2d, 2e and 3b) result in bad RR indicator, the rest provides acceptable values. This emphasizes the importance of managing the increase of the setpoint after the critical periods in order to avoid creating a new peak on the grid.

CONCLUSION

In this paper, the first step in the development of efficient space heating load control strategies, for electric baseboard heating systems widely present in Quebec, is presented. Some strategies evaluated in this study are interesting in terms of both load reduction during peak and reset periods without affecting the occupant thermal comfort. This study hence demonstrates the feasibility of possible load control strategies without using any thermal storage equipment for typical light wood-framed housing in this region. These results are valid only for the simulated building and extrapolation to the whole building stock must be done carefully. In order to do so, buildings with different characteristics should be modeled including different insulation and fenestration characteristics, infiltration rates, orientation, thermal mass, location, etc.

An experimental validation of the simulated strategies could be done using the twin houses test bench already built at the LTE site.

The building simulation could also be improved by the coupling of an airflow network model in order to evaluate the effect of the air transfer between thermal zones, with and without mechanical ventilation, on the strategies performances.

NOMENCLATURE

ACH : air changes per hour
C : thermal capacity (kWh/°C)
$E_{heating}$: energy consumed by the space heating equipements (kWh)
$E_{internal}$: internal gains (kWh)
ELA : effective leakage area (cm^2)
E_{solar} : solar gains (kWh)
h_c : internal convection coefficient (W/m^2K)
$m_{infiltration}$: infiltration (kg)
P : average power demand over the timestep (kW)
PLR : power load ratio
PPD : predicted percentage dissatisfied
RR : reset ratio
ts : time step (h)
t : time (s)
T : air temperature (°C)
$UA_{apparent}$: apparent thermal losses through the envelope and including the effect of infiltration (W/°C)
$UA_{enveloppe}$: apparent thermal losses through the envelope (W/°C)
τ : time constant (h)

REFERENCES

AEE, Fiche Aide-mémoire Novoclimat, www.aee.gouv.qc.ca, 2010

Beausoleil-Morrisson, I., The adaptive simulation of convective heat transfer at internal building surfaces, Building and Environment, 37, 2002, pp. 791-806

Braun, J.E., Chaturvedi, N., An inverse gray-box model for transient building load prediction, HVAC&Research, vol.8, no.1, January 2002.

Braun, J.E., Zhong, Z., Development and evaluation of a night ventilation precooling algorithm, Purdue University, for the California Energy Commission, August 2003.

Charron, R., Athienitis, A., Verification of a low energy solar home model to be used with a GA optimisation tool, CETC Number 2007-145, August 2007.

CRA 1995. Impact evaluation of the California Statewide pricing pilot, prepared for the California Energy Commission by CRA International, March 2005, USA

Gunther, S., Projet panne de courant, phase II: Comportement thermique des bâtiments pendant et après une panne de courant, LTE, Hydro-Québec, 2001 - confidential

Henze, G.P., Kalz, D.E., Liu, S., Experimental analysis of model-based predictive optimal control for active and passive building thermal storage inventory, HVAC&R, vol.11, no2, April 2005

Herter, K, McAuliffe, P, Rosenfeld, A., An exploratory analysis of California residential customer response to critical peak pricing of electricity, *Energy*, vol. 32, 2007

HQ, Rapport executif final sur le potential technico-économique d'amélioration de l'enveloppe thermique des habitations du

Québec, Hydro-Québec, December 1993 – confidential.

Katimpamula, S., Lu, N., Evaluation of residential HVAC control strategies for demand response programs, ASHRAE Transactions, 2006

LBNL, 2006, Demand shifting with thermal mass in large commercial buildings: field tests, simulations and audit, prepared for the California Energy Commission, CEC-500-2006-009, January 2006

Lee, K.h., Braun, J.E., Development of methods for determining demand-limiting setpoint trajectories in building using short term measurements, Building and Environment, vol.43, 2008, pp. 1755-1768.

Lu, N., Katimpamula, S., Control strategies of thermostatically controlled appliances in a competitive market, IEEE, 2005

Millette, J., Lapperrière, A., Desbiens, G., Charrette, D., Manuel technique : JAG2.0, LTE, Hydro-Québec, 2004 - confidential

Moreau A., Le Bel C., Assessment of the impact of internal gains on the thermal loads in the residential sector, Canadian Electricity Association, December 1994

Persson, T., Nordlander, S., Rönnelid, M., Electrical savings by use of wood pellet stoves and solar heating systems in electrically heated single-family houses, *Energy and buildings*, 37, 2005, pp. 920-929

PGE, Direct load control pilot for electric space heat – Pilot evaluation and impact measurement, 2004

PNNL, 2007. Pacific Northwest GridWiseTM Testbed Demonstration Projects, Part I. Olympic Peninsula Project, prepared for the U.S. Department of Energy, USA.

Reddy, T.A., Norford, L.K., Kempton, W., Shaving residential air-conditioner electricity peaks by intelligent use of the building thermal mass, energy, vol.16, no7, 1991, pp.1001-1010

Yang, L., Li, Y., Cooling load reduction by using thermal mass and night ventilation, Energy and Buildings, 40, 2008, pp. 2052-2058.

Yin, R., Xu, P., Piette, M.A., Kiliccote, S., Study on Auto-DR and pre-cooling of commercial buildings with thermal mass in California, Energy and Buildings, vol42, no7, July 2010, pp.967-975.